A Condensed version of this paper was presented to the Particle Accelerator Conference, Chicago, Ill., March 1-13, 1971

UCRL-20452
Preprint

A 3-MeV INJECTOR FOR THE SUPERHILAC

D. A. Spence, B. F. Gavin, R. Peters,
L. L. Reginato, B. H. Smith, and R. C. Wolgast

June 1971

AEC Contract No. W-7405-eng-48

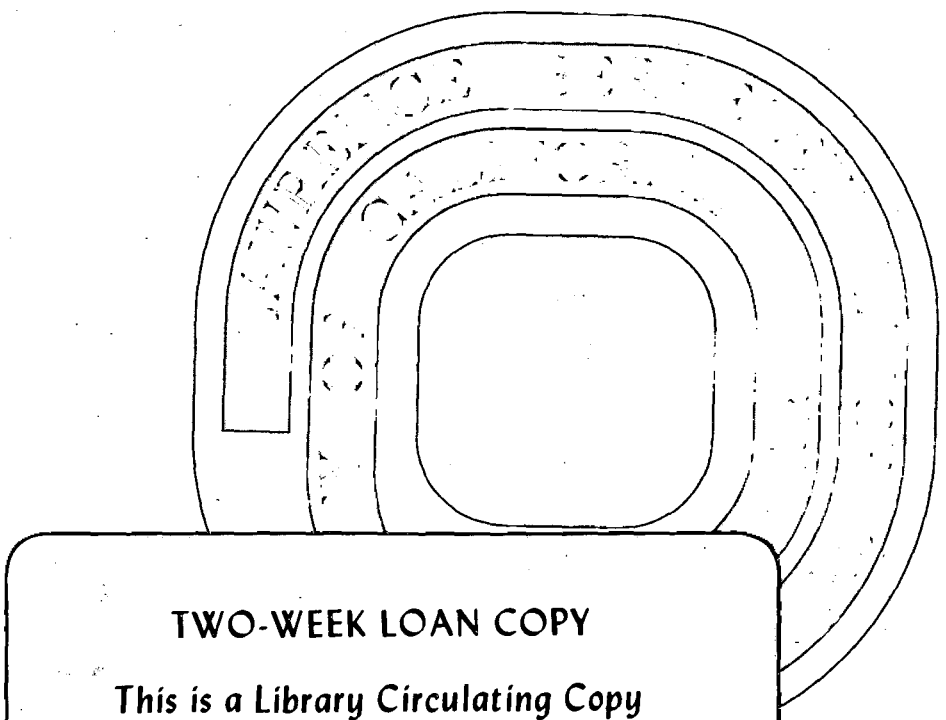

UCRL-20452

DISCLAIMER

A 3-MEV INJECTOR FOR THE SUPERHILAC*

D. A. Spence, B. F. Gavin, R. Peters,
L. L. Reginato, B. H. Smith, and R. C. Wolgast

Lawrence Radiation Laboratory
University of California
Berkeley, California 94720

June 1971

Introduction

Incorporated into the SuperHilac is a new pressurized high-voltage generator which accelerates multiply-charged heavy ions with charge-to-mass ratios between 0.042 and 0.09. This injector, a shunt-fed Cockcroft-Walton[1-3] of the dynamitron type, will be used in addition to a modified version of the existing Cockcroft-Walton which has served as the Hilac injector until the present time. Both injectors can operate simultaneously, using alternate pulses in the linac cavities. The two heavy-ion beams, each with β=0.0155 but with differing charge-to-mass ratios, will enter the prestripper tank of the SuperHilac under control of a rapid cycling switching magnet. Subsequent acceleration in the linac is done with a total of eight Alvarez cavities, two in the prestripper and six in the poststripper tank. A solid-foil stripper will be located between the two tanks.

The new injector uses silicon diodes in its voltage multiplier operating at 100 kHz. Spark protection is afforded by electrostatic shields, spark gaps, and current-limiting resistors. Peak heavy-ion currents of 15 mA at duty factors up to 50% can be supplied. A mixture of 80% N_2 and 20% CO_2 is contained in the pressure vessel at 250 psi.

The accelerating tube is 8 ft long and is constructed of pyrex-glass insulators and stainless steel electrodes with O-ring vacuum seals. It is supported in a cantilevered structure which is 18 ft long, including the 2000-lb

high-voltage terminal.

Space limitations in the HV terminal have made necessary the development of all-new solid-state ion source electronics, and have required beam transport magnets of minimum weight and power consumption. The arc and extractor power supplies are Kerns-type regulators [Q. A. Kerns, Rectifier System, U. S. Patent No. 2,579,235 (Dec. 8, 1951)]. The beam transport system consists of a 129° analyzing magnet which contains the source, a quadrupole doublet, and a vernier bending magnet. The analyzing and quadrupole magnets have tape-wound coils, and the power supplies are SCR-controlled with current regulation. The ion source has ferrous steel cathode holders, which are liquid-freon cooled, a spinning-formed tantalum anode, and utilizes plasma-heated cathodes in a P.I.G. discharge. A cryogenic pump with two cold finger stations pumps all gases except hydrogen, helium, and neon, which are pumped through the accelerating tube.

Communication with the terminal at high voltage is done with a telemetry system using infrared light beams in a PCM configuration that provides 192 "ON-OFF" and 16 analog channels. Local control is provided on all systems to allow testing and maintenance to be performed with the pressure vessel retracted.

Mechanical Design

Pressure Tank

The injector consists of a horizontal cylindrical tank 8 ft in diameter and 20 ft long with 11/16-in. walls (Fig. 1). It weighs 18 tons. Rails have been provided to retract the pressure cylinder from the 7-in.-thick stationary end door. This motion is done with a hydraulic cylinder. Opening the tank takes only a minute since a quick-acting hydraulically powered door lock is used.

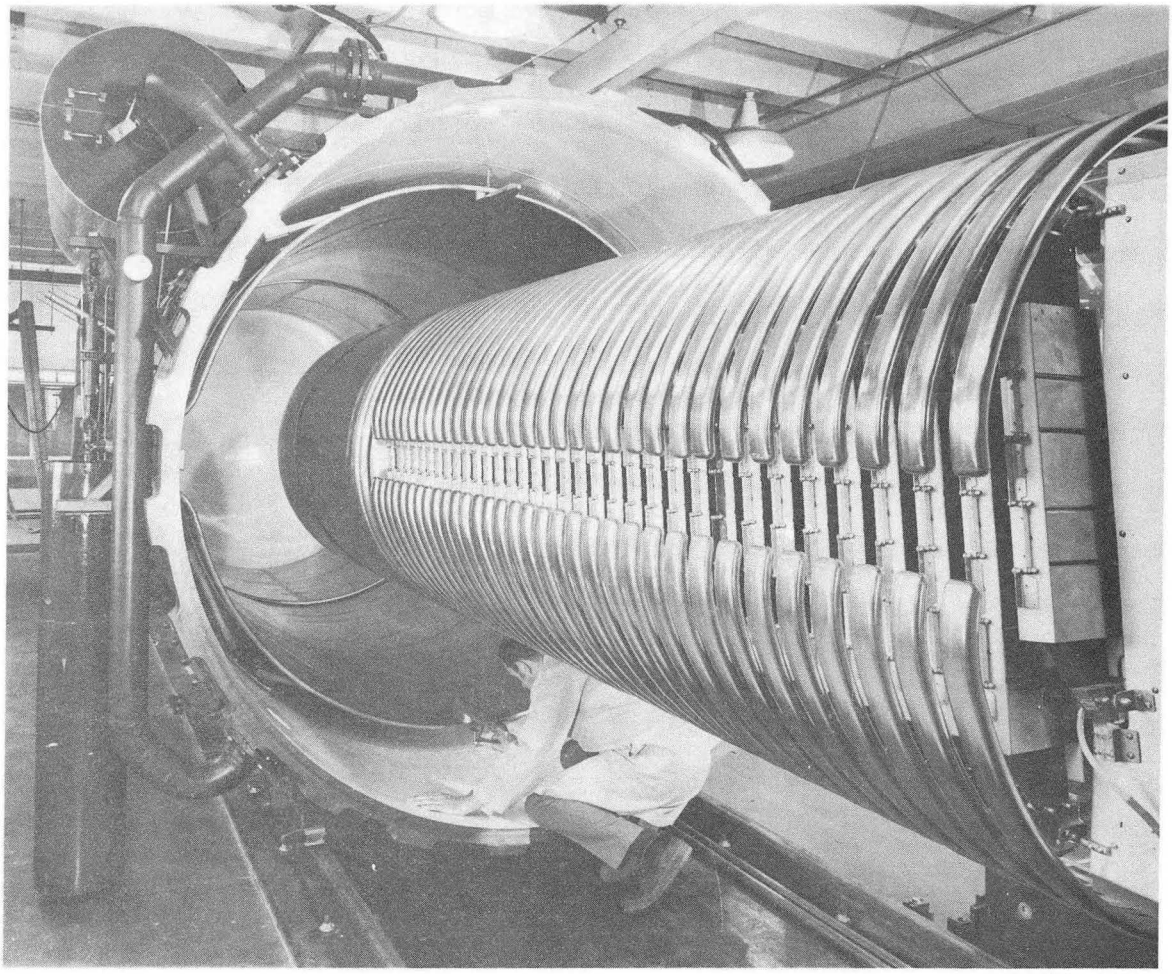

CBB709-4049

Fig. 1. The 3-MV injector with the pressure tank retracted.

Tank Insulating Gas

The tank is filled with an insulating gas, at a pressure of 250 psi, composed of 80% N_2 and 20% CO_2. This gas is released to the atmosphere whenever the tank is opened. To reduce the residual atmospheric oxygen content in the insulating gas, the tank is purged by filling to 50 psi with N_2 and then dumping. This is done three times. The fourth time the tank is filled with CO_2 to a pressure of 50 psi and then filled with N_2 to a total pressure of 250 psi. The gases are stored in liquid form at a pressure of 300 psi and are boiled and warmed to room temperature before they enter the tank. Total turn-around time is about 1-1/4 hr: purging takes 15 to 20 min; filling, about 45; and dumping requires 5 or 10 min (depending on how much noise is acceptable).

Terminal Power

Power in the terminal is provided by two brushless alternators: output from the first one is 840 Hz, 208 V, 20 kVA, and from the other, mounted on the same shaft, 60 Hz, 110 V, and 3 kVA. They are driven by a solid delrin plastic shaft 1-1/2 in. in diameter, rotating at 3600 rpm, and driven by a 50-hp electric motor outside the tank. The plastic shaft is unable to withstand high stresses induced during start-up if the motor is connected directly to the 480-V supply. Start-up voltage is therefore limited to 300 V. This provides enough acceleration to bring the alternators up to speed in 5 or 6 sec without overstraining the shaft.

The shaft, about 9 ft long, has a total of 8 steel, sealed ball bearings along its length. The aluminum blocks in which the ball bearings are mounted are cooled by liquid freon and operate at room temperature. Without cooling, the bearings in quiet air at one atmosphere will reach a temperature of 250°F,

which is a little marginal for the plastic shaft.

A commercially available mechanical seal (Crane Packing Co. type 1 B Double) with sliding surfaces is used on the shaft at the tank wall. This seal runs in a water-cooled bath of oil.

The bearings along the shaft were installed along an optical line of sight so that when the high-voltage terminal is fully loaded, producing a deflection in the support structure of 3/4 in., the shaft is in a straight line.

Cooling

The heat produced by rf losses in the tank is removed by circulating the insulating gas and passing it through heat exchangers outside the tank.

The heat produced by the ion source and its auxiliaries in the terminal is removed by circulating liquid freon TF. The freon is refrigerated to 50°F at a pressure of one atmosphere outside the tank and piped to the HV terminal in an ungraded nylon pipe (1 in. i.d. x 1/4 in. wall x 9 ft long). After abstracting heat from the terminal components the freon is returned, still in liquid form at 90°F, through another nylon pipe back to ground. There has been one electrical discharge through the liquid freon, and it broke the nylon. Tests indicate that the discharge occurred because the freon was badly contaminated.

Accelerating Tube

The accelerating tube is 8 ft long and has 77 electrodes. The electrodes are 1/16 stainless steel, with a 4-in. hole, and separated by pyrex-glass insulators about 1 in. thick. Each electrode has an O-ring vacuum seal against each face. This permits the entire tube to be disassembled for cleaning. Six delrin rods under tension provide the compression to keep the tube straight

when it is horizontal and supported only at the ends (Fig. 2).

Electrical Design

Diodes

Our experience with silicon diodes in series-fed Cockcroft-Walton rectifiers indicates that they posses much higher reliability than other types of rectifiers. Since an outage of the 3-MV injector interrupts the operation of the entire SuperHilac, it seems highly desirable to include this advantage in the injector even though it incurred the expense of an R & D program.

Our preliminary studies evaluated the performance at 100 kHz. Most manufacturers produce small high-voltage modules rated at about 10 kV which contain 15 or 20 PN junctions encapsulated in plastic. We found that these did not perform as well as assemblies made up of individual junctions, for two reasons. First, at 100 kHz, the energy dissipated per junction is appreciable and the plastic encapsulation inhibits the heat flow away from the junction, limiting the current capability of the rectifier. Secondly, the capacitance shunting each junction was not large enough to control the inverse voltage in the presence of the large displacement currents penetrating the case longitudinally in a 3-million-volt sparking environment.

Of the individual diodes we tested, the Unitrode UT-71 seemed to be the best compromise between current capability and resistance to sparking transients. Some of the higher speed diodes handled slightly more current but were much more easily damaged by sparking surges.

After studying the geometry of the 3-MV injector, we concluded that during sparking the discharge was likely to be oscillatory with a frequency of about 10 MHz. The estimated surge impedance of the circuit indicate that the

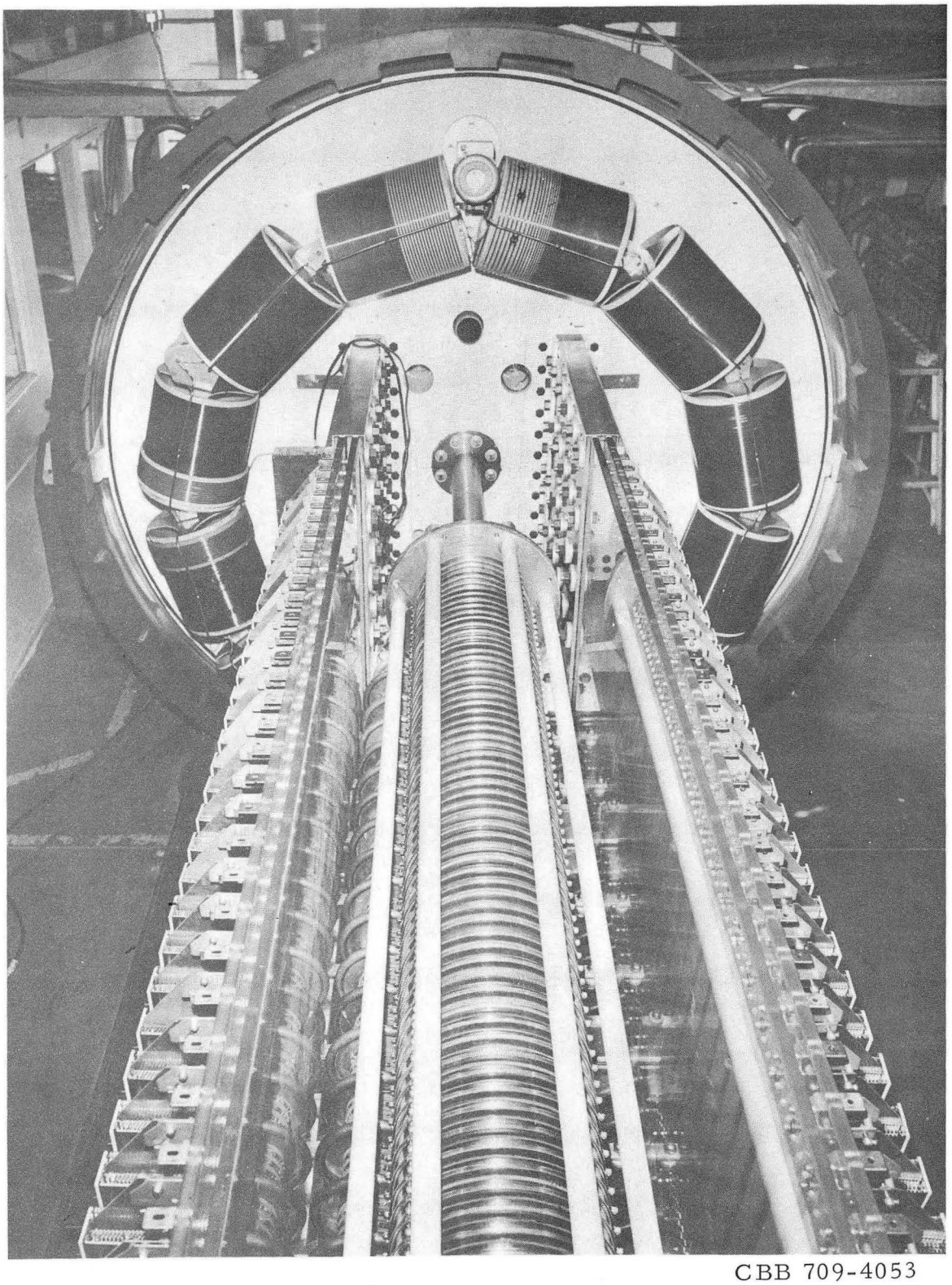

CBB 709-4053

Fig. 2. The accelerating tube installed in the horizontal support structure.

peak current would be limited to about 20,000 A.

For our tests a tank about 24 in. in diameter by 3 ft tall was assembled in which we could contain the same atmosphere and pressure that the injector would use. A small 300-kV, series-fed Cockcroft-Walton rectifier was suspended from the top of the tank as a source of voltage and we arranged the geometry so that the ringing frequency would be 10 MHz and the surge currents about 20 kA. With this test setup we determined that the peak forward current through the test diode would have to be limited to about 100 A.

Test diodes were mounted on an etched circuit board with protective spark gaps connected across the assembly to limit the peak voltage that could be applied. The current was limited to 100 A by connecting resistors in series with the diode string. In this atmophere such spark gaps fire in less than 1 nsec.

The polarity of the test diodes was then reversed, and the spark gap limited the voltage across the assembly to well within the diodes' avalanche potential. However, the diodes failed consistently in test after test. It seemed that no matter what we did to the gaps the diodes always failed. Finally we mounted a set of diodes on the board with their terminals connected to nothing but their protective capacitors. The diodes still failed. Apparently the displacement currents associated with the rapidly changing and intense electric fields were sufficient to break the diodes down in spite of the fact that we had increased the diode shunting capacitance to the maximum which we could tolerate in the injector. The electric fields were not coming from the potentials associated with the protective spark gaps but were coming from the 300-kV source. After shielding the assembly from these intense external fields, the diode failures ceased. We concluded that there are three things which have

to be done to protect silicon diodes operating in MV machines. First, spark gaps have to be employed to restrict the inverse voltage that can be applied to the diode during sparking. Secondly, resistors have to be connected in series with the diodes to limit the peak currents to about 100 A. And thirdly, the diode assemblies have to be shielded from intense and rapidly changing electric fields.

The diode assembly used in the injector is shown in Fig. 3. The adequacy of these protective techniques has been confirmed by operation of the injector at voltages up to 3-1/4 million volts with thousands of sparkdowns without the loss of a single diode. Figure 4 shows the diode assemblies installed.

The Electrical System of the Shunt-Fed Cockcroft-Walton

Figure 5 shows the circuit diagram of the 100-kHz rf system. The oscillator is a modified Colpitts circuit. The resonant circuit consists of 12 solenoids mounted in such a way as to provide a toroidal coil (Fig. 6). The semicylindrical electrodes (dees) couple rf to the corona rings and provide the capacitance necessary to tune the coil to 100 kHz. The center-tap of the toroidal inductor is not grounded, so that there is only one path for the rf circulating current to flow and this is through both dee capacitances. Thus the dee-to-ground voltages are equal to an accuracy determined by the relative dee-to-ground capacitances.

The anode of the Eimac 4 CW 100,000 is inductively coupled to the toroidal inductor with a step-up ratio of 10 to 1, producing a dee-to-dee voltage of 350 kV. The oscillator is capable of delivering 200 kW of rf power, although at 3 MV and no beam load the dc power input to the oscillator is 47 kW. The grid excitation is obtained from a capacitive divider from dee to ground.

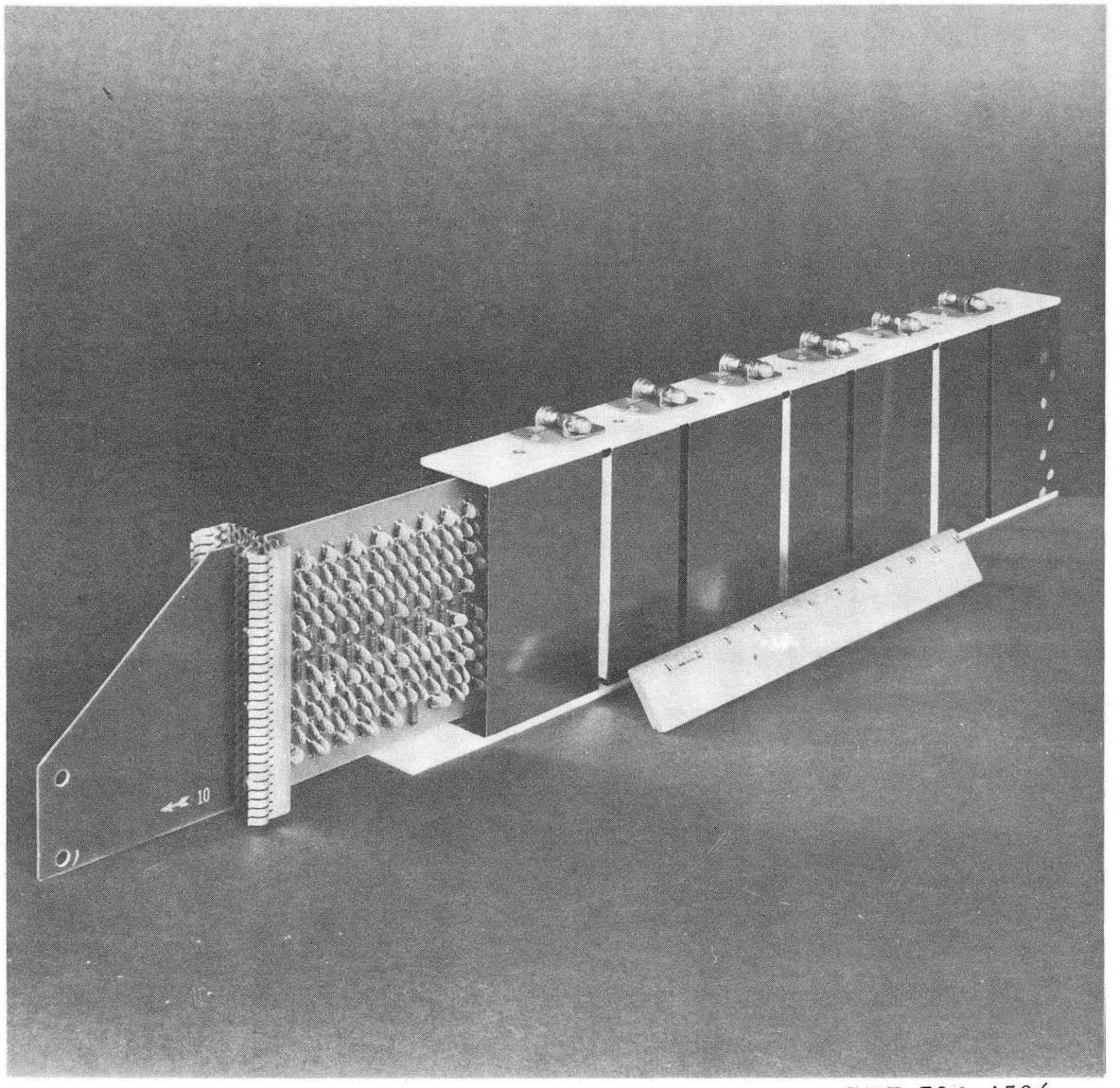

CBB 703-1506

Fig. 3. Diode board partially removed from shielding assembly.

CBB 703-1273

Fig. 4. A few diode assemblies and corona rings installed.

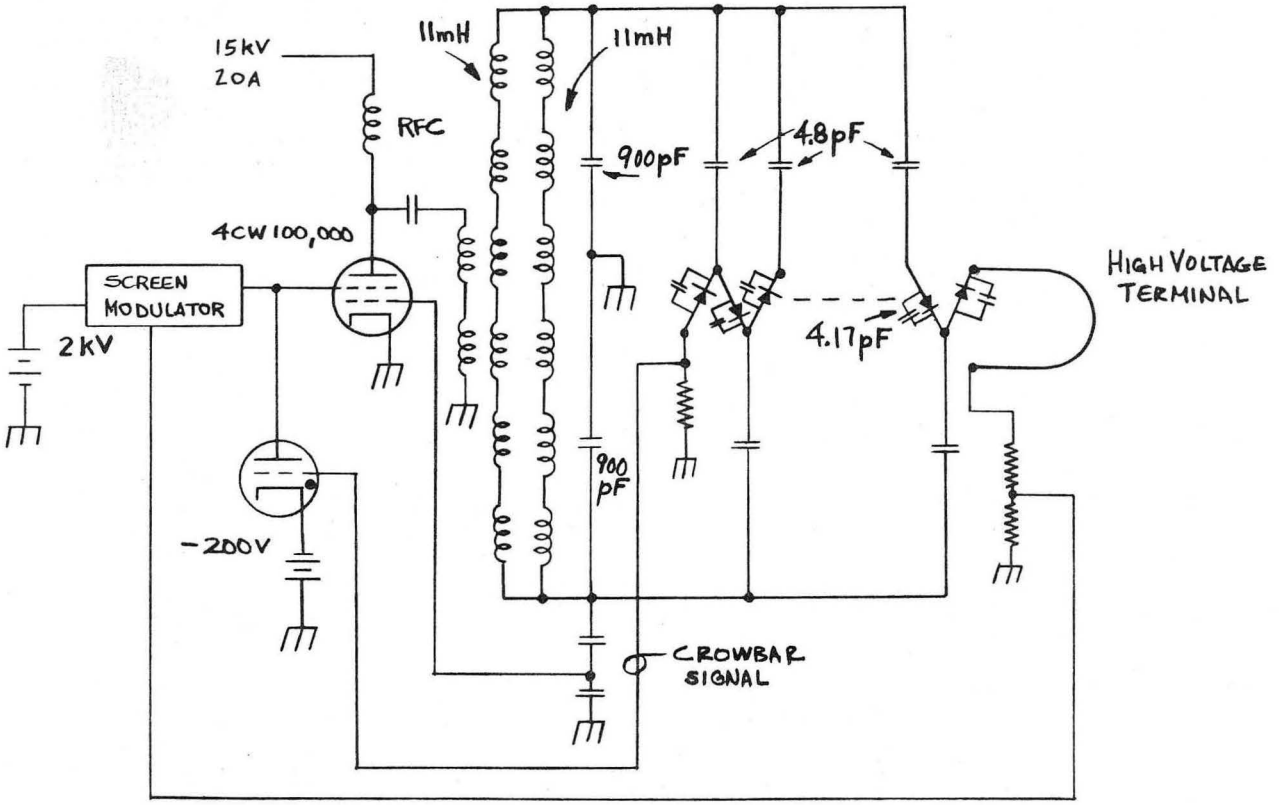

Fig. 5. Circuit diagram of the 100-kHz of rf system.

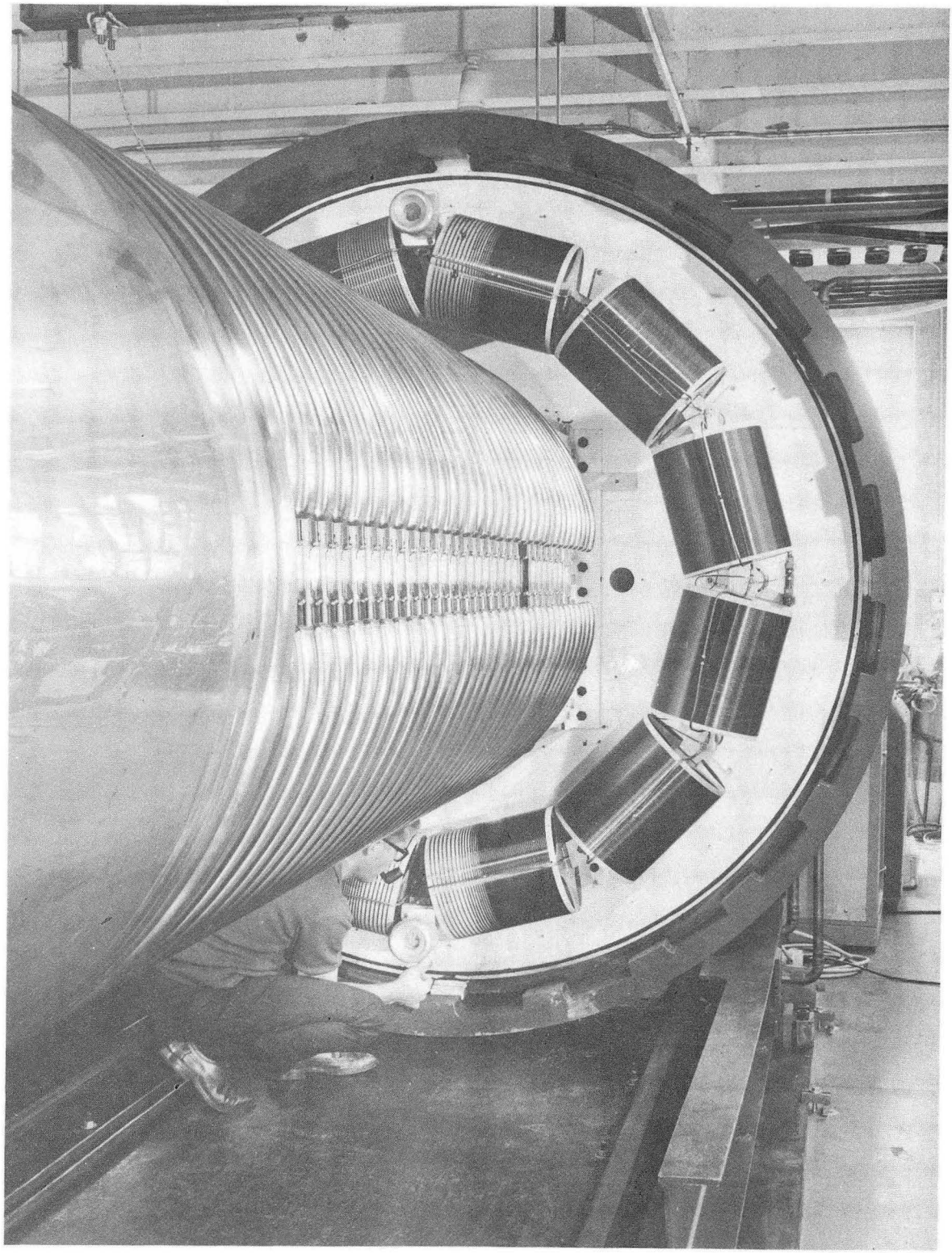

CBB 709-4051

Fig. 6. Twelve solenoids are mounted on the stationary end door. Note the protective spark gaps on each coil.

We found that it was necessary to protect the toroidal coils with spark gaps and to provide a high resistance drain from coil to ground to remove charge accumulating on the dees.

High-speed over-current protection is provided by a crowbar operating on the oscillator screen grid. It stops power flow within a few microseconds of an overcurrent. The output of the 3 MV power supply is regulated by modulating the screen grid.

Telemetry

In order to carry out the many control functions associated with the ion source electronics, an optical communication system using a pulse code modulation (PCM) format has been designed.[4] This system handles 16 analog channels and 192 "ON-OFF" channels which are sampled and transmitted with each machine pulse. One optical link is used to send clock information from the ground end to the terminal so that the data transmitters and receivers will be synchronized. The second optical link sends PCM data up to the terminal, while a third optical link sends PCM data from terminal to ground. In addition to the PCM data channels, there are also two analog optical channels which continuously monitor arc current and extractor potential in the ion source.

Special precautions were taken in the terminal portion of the telemetry to protect the delicate integrated circuits from 3-MV spark-induced transients. These precautions include double shielding, input and output isolation with either photon decouplers for analog or fast pulsed data, or relays for switch data. All low-frequency inputs and outputs have rf filters. Lines that cannot have RC filtering because of frequency requirements have fast transient suppressors instead. The injector has been sparked many times at 3 MV without the loss of any integrated circuits.

High-Voltage Terminal

High-Voltage Terminal Size

The high-voltage terminal is covered with a 0.025-in. stainless steel shell 4 ft diameter by 6 ft long. The terminal fully loaded weighs about 2000 lb. It is supported from the stationary door of the tank on an insulating beam built up of 3/4-in. plexiglass plates. An exposed view of the terminal is shown in Fig. 7.

Ion Source Magnet

The ion source magnet performs a dual role. It provides a field of 2.85 kG or more for the ion source in a magnetic gap of 2.2 in. and a field of 4.75 to 7.66 kG to analyze and focus the beam in a gap of 1.42 in. The embryonic shape of the magnet stems from the need to keep the power and size down. The pole sides were cut 0.44 gap lengths wider on each side than the outermost beam path. The field at this width is 97 to 99% of the centerline field. The pole exit edge is cut at an angle of 36.75° with respect to the normal to the beam path, to provide vertical focusing. The magnet weighs 480 lb and uses 2400 W at full field. The coils are cooled by conduction through the yokes. Each yoke was made of two plates brazed together to form a broad coolant passage. The coils are electrically insulated by 0.005-in.-thick alumina, plasma-sprayed onto the yokes. The poles are welded to 0.25-in.-thick stainless steel plate to form the vacuum chamber. The heavy walls are needed to withstand the 250 psi of insulating gas. The coils are held tightly against the yokes with a rubber shim placed between them on the median plane. Appropriate cutouts were made in the coils to provide clearance for the ion source and the emerging beam. Figure 8 is a cross-section schematic of the magnet construction.

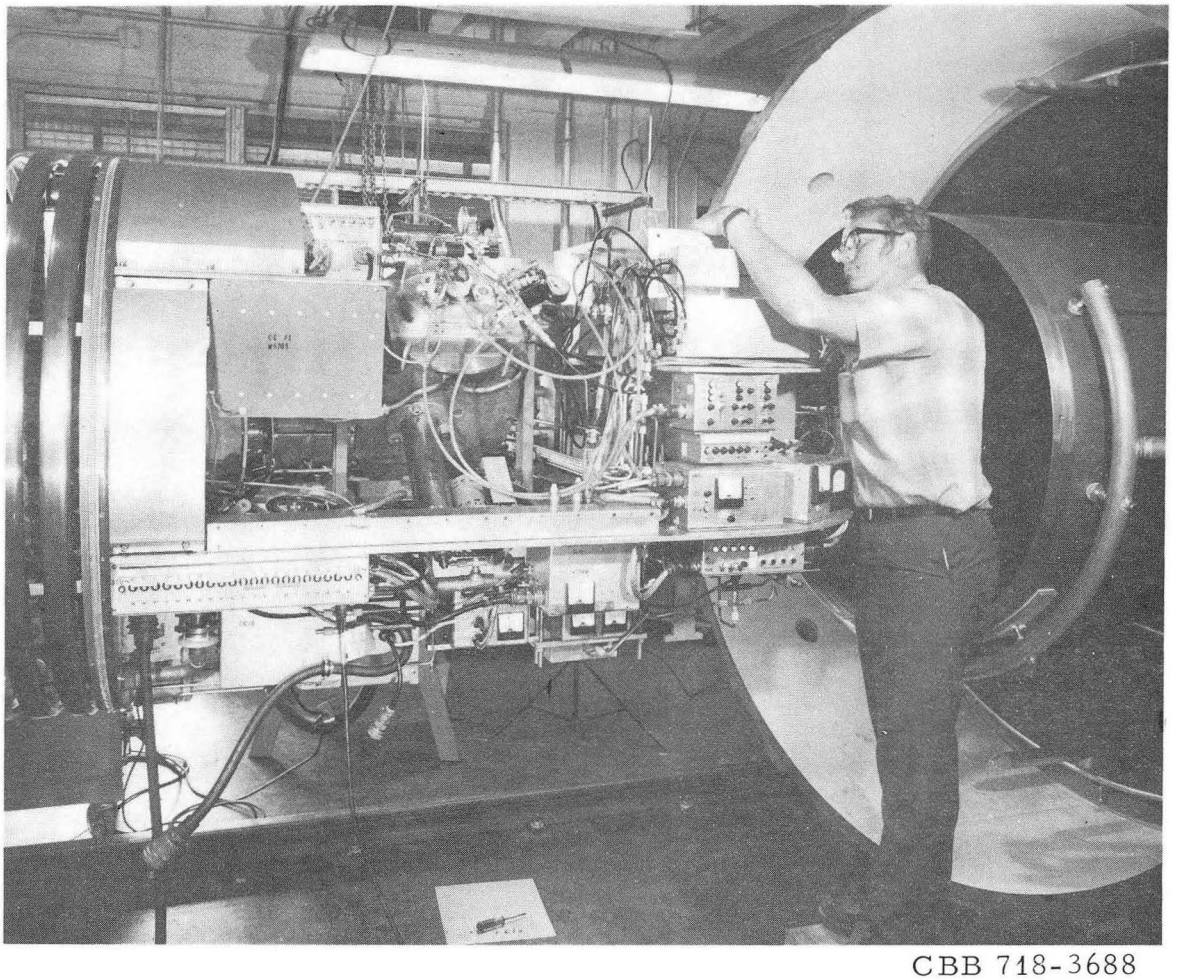

CBB 718-3688

Fig. 7. High-voltage terminal with shell removed.

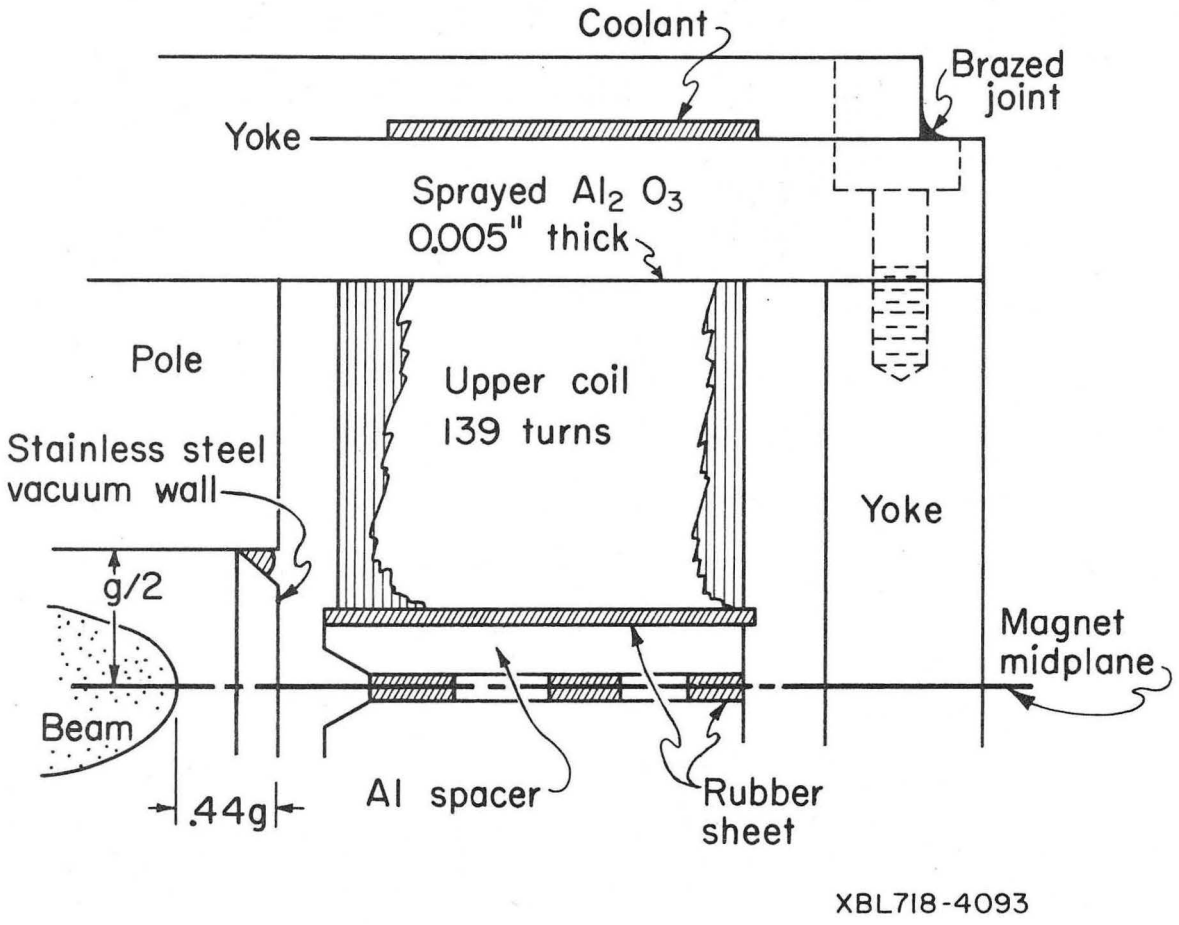

Fig. 8. Schematic cross-section of the ion source magnet.

Vacuum System Description

Two coldfingers differentially cryopump the heavy ion source. One coldfinger near the source freezes most of the source gas load and provides adequate clean vacuum for source operation. The second coldfinger near the beam entrance into the high voltage column produces high vacuum to reduce ion beam loss through charge exchange and accidental electrical discharges. The $20^{\circ}K$ temperature is produced by a small refrigerator in the terminal and is transmitted to the coldfingers by hydrogen-charged heat pipes. Feasibility tests of various cryopump configurations using this model refrigerator were conducted by N. Milleron.

At $20^{\circ}K$ all gases have vapor pressures less than 10^{-10} mm Hg except hydrogen, helium, and neon. There is no substantial steady load of these gases in the system, so they can be left to pass down the accelerating column to pumps at ground potential. The conductance of the column is about 33 liters/sec for air (for hydrogen, 125 liters/sec; helium, 88; neon, 39). If these light gases are needed as a source of ions they will be run in the low voltage (750 kV) injector with its own pumping system. The next most volatile gas is nitrogen, with a vapor pressure of 10^{-7} at $25.2^{\circ}K$, closely followed by several other gases, which sets an upper limit on the coldfinger operating temperature.

Figure 9 shows a layout of the ion source and beam transport system in the terminal. The ion source vacuum chamber in the magnet uses the magnet poles as part of the envelope welded to stainless steel plate. Rectangular ducts pass through cutouts in the magnet coil to provide for insertion of the ion source and for the beam exit.

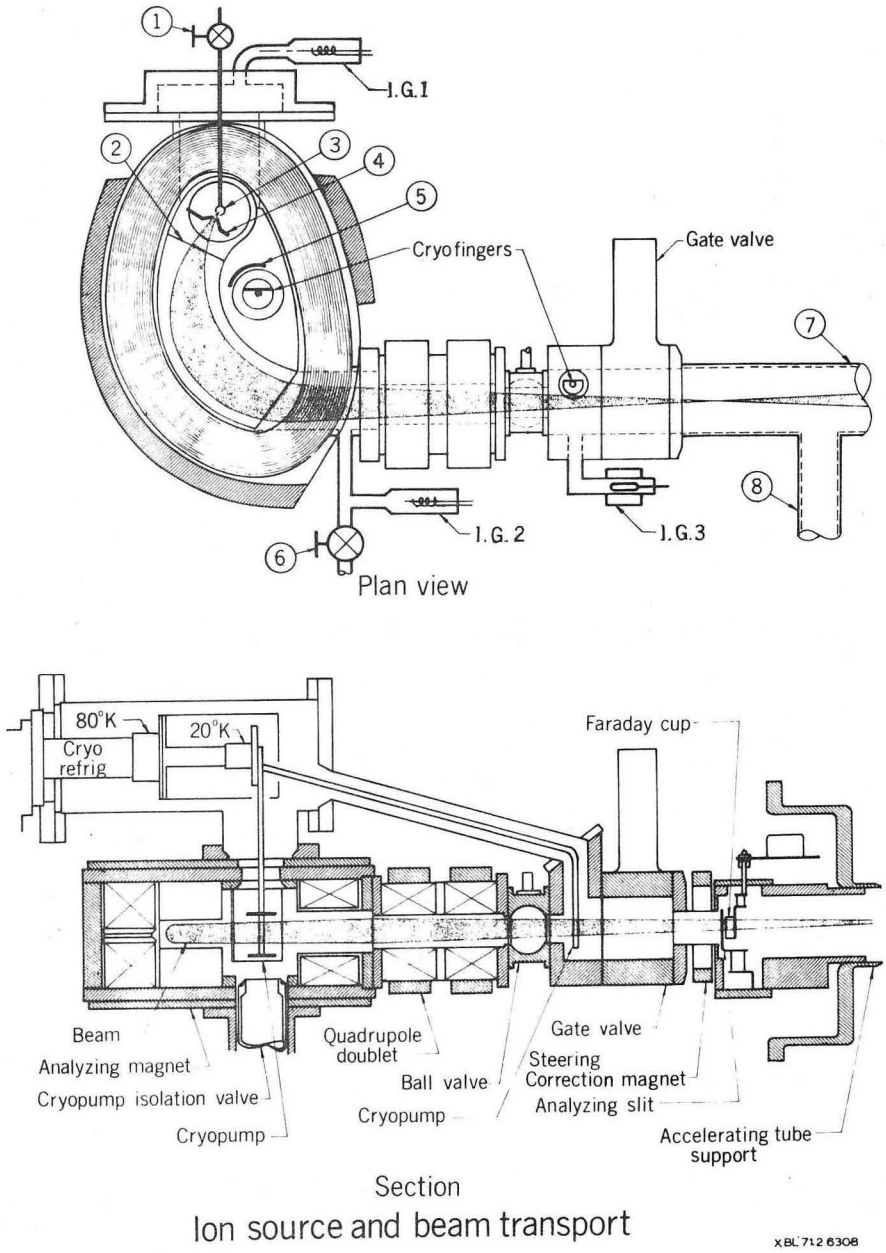

Fig. 9. The plan view shows the system as set up for vacuum tests and beam focussing measurements. 1: leak valve; 2: step in the magnet pole from 2.9-in. gap on the ion source side to 1.42-in. gap; 3: ion source anode; 4: ion source extractor (0.8 in. high); 5: radiant heat shield; 6: roughing valve; 7: tube-to-beam measuring slits; 8: outlet to 2-in. diffusion pump. Ion gages I.G. 1 and 2 are model VG-1A. I.G. 3 is a Penning-type model GPH-001. The elevation view in section shows additional components to be installed for operation in the injector.

A 2-in. diffusion pump was mounted temporarily onto the system to stand-in for the pumping capacity to become available through the accelerating column. It was partially baffled by a 2-in. opaque water-cooled elbow. Elastomer seals are used throughout the system.

The first coldfinger is inserted into the deep crescent-shaped space between the magnet poles and coil. The finger was formed by the .25-in.-diam copper-tube heat pipe to which two 1.5-in.-diam copper discs are soldered. The discs are mounted above and below the magnet gap to avoid intercepting stray beam and thermal radiation from the ion source. The tantalum anode of the ion sources operates at a bright orange temperature and radiates about 500 W. A liquid-Freon-cooled radiation shield intercepts the direct radiation from the source. The walls of the crescent-shaped space are lined with cooled copper to intercept as much as possible of the diffuse radiation without as much as possible of the diffuse radiation without impeding the molecular gas flow. Both shields are chemically blackened. The coolant temperature is about 15°C. The second coldfinger was just the .25-inch-diam heat pipe. Our initial operation showed there was some excess refrigeration capacity so the coldfinger areas were increased. A vertical copper sheet was added between the discs of the first, and a 1.0 x 3.25-in.sheet to the second. The total exposed areas now are 15.6 $in.^2$ and 7.3 $in.^2$.

Each gravity flow "heat pipe" is supplied with hydrogen through a fine tube from a separate 15-$in.^3$ reservoir at room temperature. The hydrogen liquefies at the cold head of the refrigerator and runs down the coldfinger, hastening the cooldown and maintaining a low temperature drop under the heat load. The reservoir is initially charged to 100 psi to provide enough hydrogen to make about 1 in. of liquid in the .25-in. tube. Each reservoir

is fitted with a bourdon gage to serve as a vapor bulb thermometer after some liquid has formed, at pressures below 60 psi in this case. The reservoirs are also fitted with pressure transducers so the pressures can be monitored during injector operation. Figure 10 shows the two coldfingers and one of the hydrogen reservoirs mounted on the cold head vacuum jacket.

Five layers of aluminized Mylar are wrapped over the 20°K cold head and the heat pipes to the point where they enter the vacuum chamber. A copper shield from the 80°K cold head shields the 20°K head. Five more layers of aluminized Mylar are wrapped over the copper shield.

The cryopump isolation valve and the ball valve allow us to isolate the cryopump so it can be kept in operation while the source chamber is let up to atmosphere (which may in the future be the 250-psi insulating gas atmosphere) for changing the ion source. The gate valve allows us to keep the accelerating column under vacuum while the cryopump is thermally cycled to remove the accumulated gas load.

The cryogenic refrigerator, the Cryodyne Model 350 (Cryo. Tech. Inc.), uses helium as the working fluid and has two stages at 80°K and 20°K. According to the production check, with a 5-W load on the first stage, the second stage capacity is 4 W at 21.8°K, 2 W at 16.7°K, and 0.0 W at 13.6°K. The production check is run with the cold head bare.

The compressor assembly was adapted from air to liquid cooling by putting liquid-cooled straps around the compressor and putting liquid-gas head exchangers in the discharge line. A plan view of the assembly, ready to install in the terminal, is shown in Fig. 11. The short tank is the oil separator and the long tank is the oil vapor charcoal absorber trap. Space occupied by the assembly is 13 x 19 x 27 $in.^3$. Space occupied by the refrigerator expander

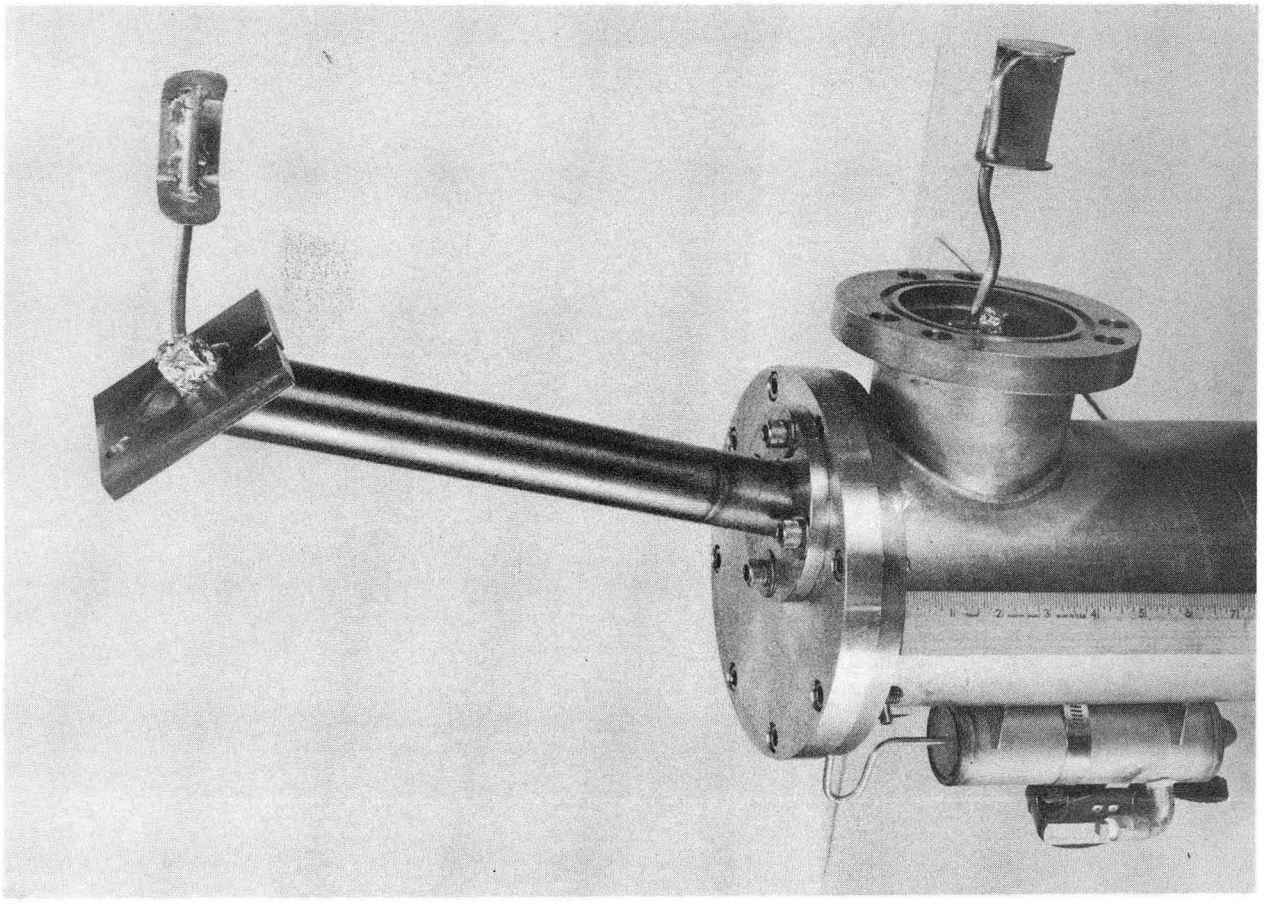

CBB 7011-5238

Fig. 10. Coldfingers attached to the refrigerator. Cold head in its vacuum jacket.

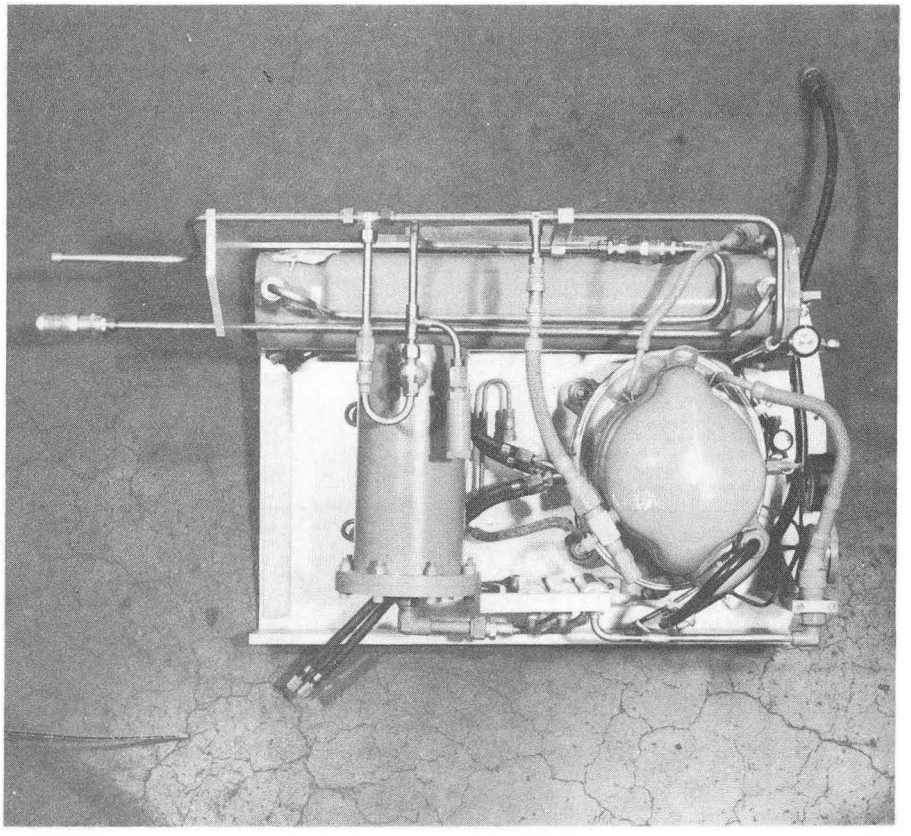

XBB 7010-4683

Fig. 11. Plan view of the modified compressor assembly.

and cold head in its vacuum jacket is 9 in. diam x 22 in. long. The refrigerator system uses 1300 W of 60-Hz power.

The operational system in the injector will provide for remote reading of the coldfinger pressures, compressor suction and discharge pressures, an ion gage, and a thermocouple vacuum gage. Remote control of the valves will be provided subject to interlocks from the gages. Plans call for the changing of ion sources through a pressure lock so the tank insulating gas need not be dumped. This would shorten the source change time from about 1-1/2 hr to 20 min.

Pumping Speed Measurements

During the air speed measurements the diffusion pump was throttled to a measured speed of less than 3 liters/sec. Gas was admitted to the system through the operational ion source by using the ion source valve to control the flow. In making the measurement for air, a burette-and-stop-watch flow measurement was used in series with a Hastings thermocouple flowmeter. The two flowmetering methods agreed within 5%. Pressures at the three ion gages were recorded. The base pressures with no flow ere subtracted and the pressure rise due to the flow was plotted in Fig. 12. Using the values from Ion Gage 1, the effective system speed for air at the source was found to be 186 liters/sec. The speed before the coldfinger areas were increased was 140 liters/sec (dashed line).

Pumping speed for argon was measured in the same way, except only the Hastings flowmeter was used. The data is plotted in Fig. 13 before applying the sensitivity factors for argon relative to air for the flowmeter and the ion gages. (Meter reading) x (1.43) = flow of argon. (Ion gage reading) x .617 = pressure of argon (Ref. 5). Applying these factors, we find the

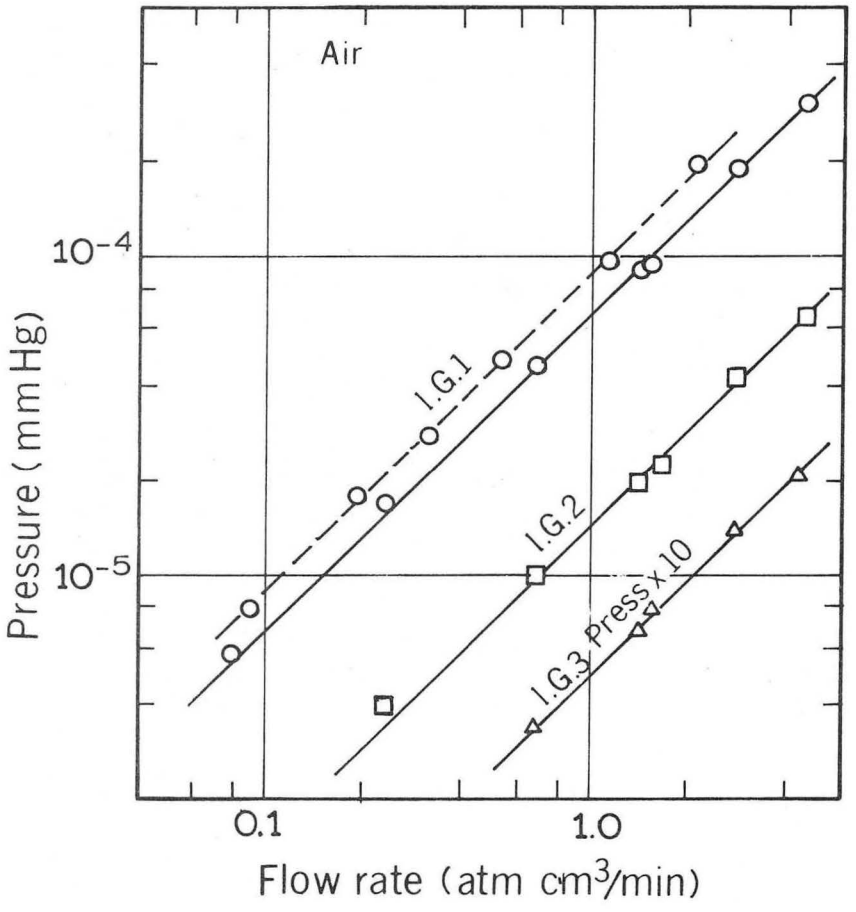

Fig. 12. Air pumping speed data: pressure rise due to flow vs flow rate.

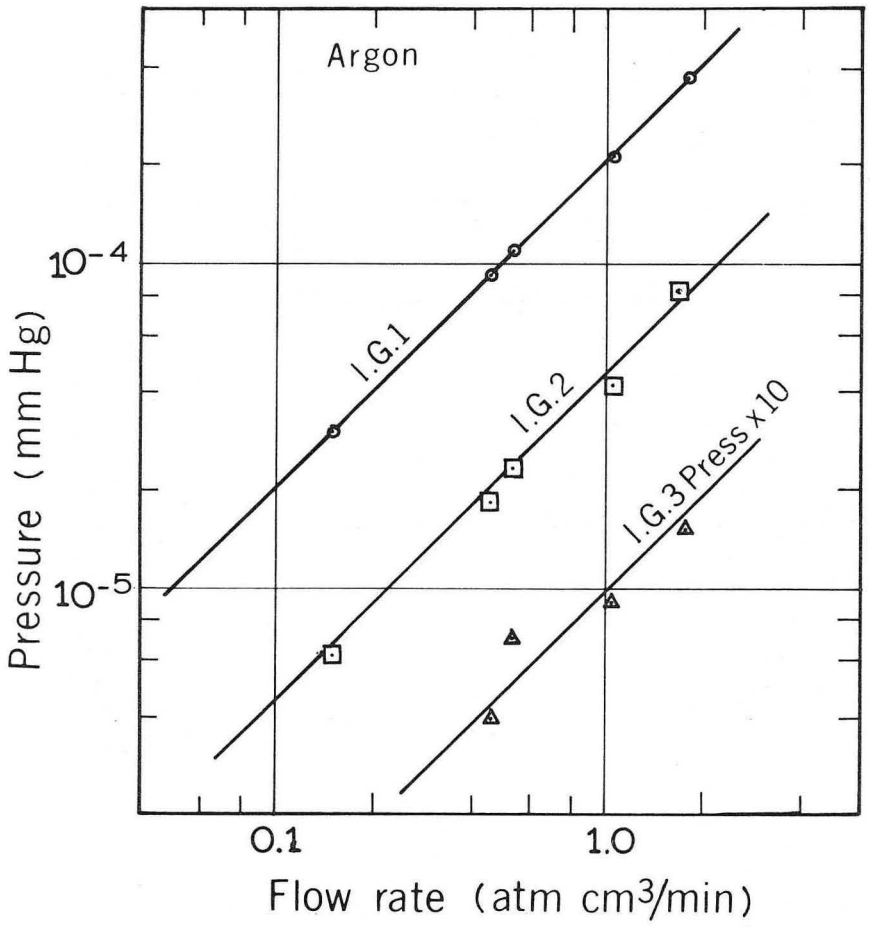

XBL 712 6306

Fig. 13. Argon pumping speed data: pressure rise due to flow rate (ion gage and flowmeter readings not corrected for sensitivity factors for argon.

effective system speed for argon to be 143 liters/sec. This value may be used to predict the speed for air if it is multiplied by the ratio of the average molecular speeds of air relative to argon (i.e., 1.18) and possible small effects of differences of sticking coefficients are neglected. Doing this, we predict an air speed of 169 liters/sec, slightly less than our measured speed of 186 liters/sec.

Vacuum Performance with Operating Ion Source

A momentary high gas flow is required to start the ion source arc, which causes no operational difficulties. After the arc is started it heats the tantalum anode to a bright orange, and the cathodes become still hotter. At this time large quantities of hydrogen are evolved, raising the vacuum pressure sometimes in excess of 10^{-3} mm Hg. This gas load quickly begins to fall until after a half hour or so this gas amounts to 10 or 20% of the gas flow being supplied to the source. Since the gas is largely hydrogen, it increases the pressures along the entire injector beam path and could cause a noticeable loss of beam operating time for heavy high-charge-state ions. We may want to pre-bake new source parts.

Another gas load appears when the extractor voltage is applied, sending ion beam through the system. Only one ion charge state is focussed cleanly through the system. All other charge states produced by the arc bombard the walls with 20-kV ions. This load also decreases with operating time but toward some steady value not zero. Much of this gas load is cryopumped. During our limited operation so far this gas seems to increase system pressures by about 3×10^{-6} mm Hg.

Of major interest to the heavy ion beam is the amount of gas it must

pass through. To make our best estimate of this quantity we made the plot shown in Fig. 14, where the estimated pressure distribution along the beam line is drawn, based on the three ion gage readings and the geometry. The solid line represents source operation with a large slit in the source anode (.05 x .47 inc.); the dashed line represents operation with a one-third smaller slit (.05 x .16 in.). Both sets of readings were made after several hours of operation. The integrals of pressure with distance from the curves as drawn are 2.8×10^{-3} and 1×10^{-3} mm Hg-cm for the two slit sizes. Correcting these values for the gage sensitivity for argon they become 1.75×10^{-3} and $.6 \times 10^{-3}$ mm Hg-cm.

During day-to-day operation without thermal cycling of the cryopump to remove accumulated gas, we have observed each day an increase in the cold-finger temperature. The temperature rise is caused by the increase in radiant heat absorptance caused by the thickening frost deposit. Experience so far does not tell us how often we need to purge the cryopump except that it will not be more frequent than every four operating shifts. A typical cool-down history is plotted in Fig. 15. The lowest curve is the pressure of the vapor bulb thermometer mounted on the cold head flange. The middle curve is the shorter coldfinger pressure and the highest curve is the longer coldfinger pressure.

It should be possible to purge the cryopump with only a partial warm-up. Xenon, for instance, has a vapor pressure of 1 mm Hg at 104°K. We have made one partial warm-up with a turnaround time of 1 hr, but have not yet tried for shorter purges. The cold head is equipped with 20-W and 10-W heaters on the first and second stages respectively to speed the process.

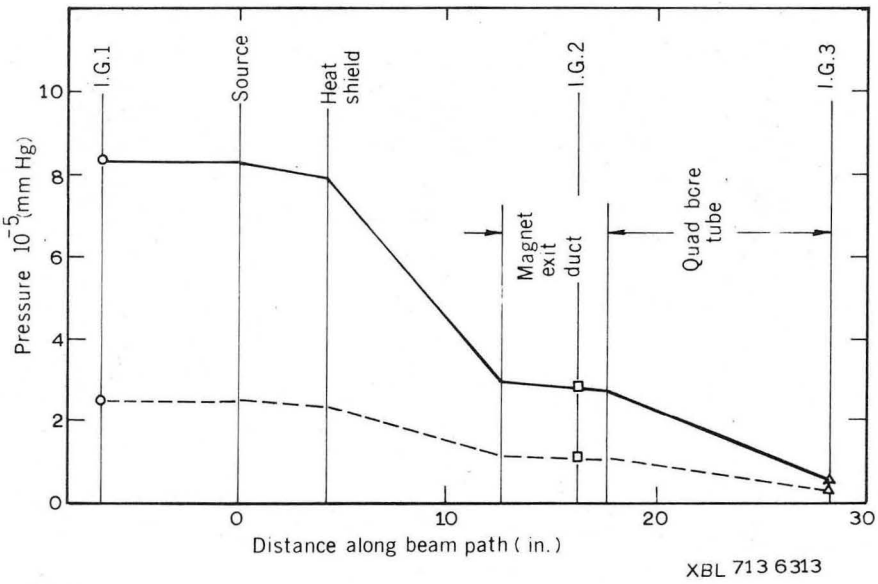

Fig. 14. Pressure along the beam line during operation with Ar^{3+} beam. Dashed line: small ion-source slit.

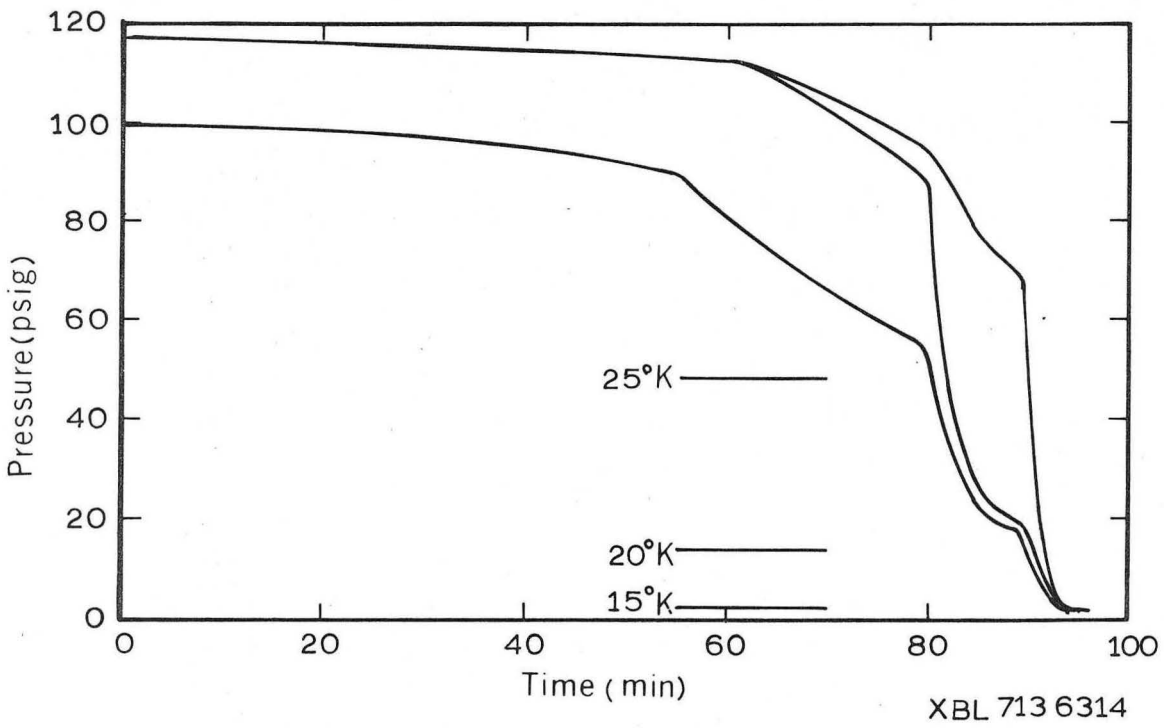

Fig. 15. Cool-down history of the coldfingers. Lowest curve is the vapor bulb thermometer pressure.

Ion Source Electronics

The heavy-ion source for the SuperHilac produces large beam currents of high charge-state ions. This requires much more massive equipment and much higher power than is customary for proton or electron sources. As a result a large high-voltage terminal is required, tightly packed with heavy components.

The extractor supply will provide potentials up to 25 kV, 100 mA. Both the arc voltage and extractor voltage are pulsed with duty factor up to 50%. Both are transistor controlled in a Kerns actuator circuit and include electronic regulators with stabilities of about 0.2% and bandwidths of about 5 kHz. The beam transport system includes an analyzing magnet and two quadrupoles, plus a small bending magnet. The magnet power supplies are of the SCR type with 0.1% regulation. All the electronic systems in the terminal employ solid-state technology in order to maximize efficiency and reliability. To reduce the size of the power transformers and the associated equipment, the ac is generated at 840 Hz.

To protect the comparatively fragile solid-state equipment from sparking transients, double shielding is used. All leads entering or leaving the second shields pass through feed-through capacitors and series resistors are connected to the leads between the first and second shields.

Ion Source Design

A Penning-type ion source is installed within a cutout portion of the main analyzing magnet. It has tantalum cathodes which are heated directly by a pulsed plasma discharge. These cathodes are almost fully recessed in small removable steel pole pieces (boats) shaped to bow the magnetic field lines in the plasma column and thereby increase the effective surface area of the

cathodes. Of late, there is fresh evidence that such bowing may have an unfavorable influence on exiting ion currents; possibly an alteration of the electron flux occurs along the magnetic field lines. (By enlarging the steel-to-steel separation on the source axis 0.25 in., the bowing can be removed entirely but would be accompanied by a 25% reduction of the magnetic field strength on this axis.) Typical anode-window-length to magnet-gap ratios are 4.5:1 for side-extraction P.I.G.s. This design could accommodate a 2.5:1 ratio.

The cathode support boats are freon cooled and serve as a heat sink for radiative cooling of the cathodes and anode (Fig. 16). In addition they reduce the magnet gap in the source region. For pulsed operation the starting voltages required by this arc are depressed by minimizing heat loss between cathode and support. These cathodes, if directly cooled, would require higher starting voltages than if allowed to quickly come to temperature. An ideal cathode would be one which could reach electron-emitting temperatures quickly but which then could be cooled more effectively so as to keep arc voltages as high as possible. A compromise has been made here. The anode is fabricated from five form-shaped tantalum parts spotwelded together. The cathode-to-cathode spacing is 1.8 in., the anode proper has a bore diameter of 0.34 in., and the side of the anode with fixed window is indented towards the bore axis about 0.01 in. The preliminary results reported here have been made with a 0.05- x 0.16-in. slit.

The extractor is grounded. Each cathode boat is insulated from ground by a 0.06-in.-thick quartz plate, the only material found to stand up to our devastating secondary electron bombardment. An external adjustment is provided to move the extractor laterally with respect to the anode slit.

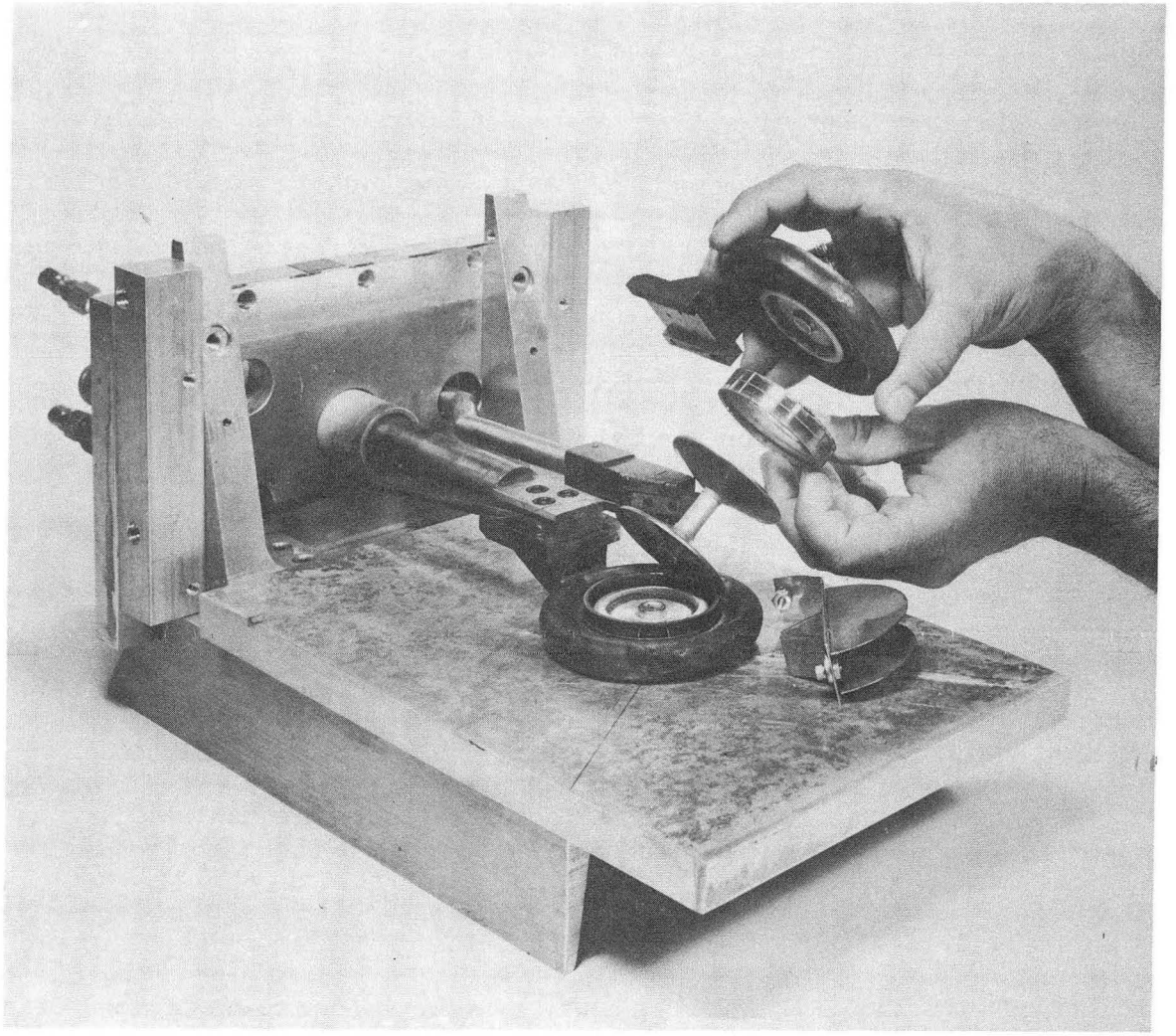

XBB 709-4058

Fig. 16. Exploded view of ion source.

The gas flow is perhaps the most critical parameter to be controlled for optimization of an ion source. We use a thermo-mechanical leak valve which has a response time of from 7-40 sec for small flow changes. A more rapid increase in arc pressure is needed for prompt arc adjustment. With this in mind we are planning to apply a short one-second burst of gas to the arc whenever arc currents drop to near zero for a certain designated period of time within any arc pulse. This superposition will trigger a small incremental increase of flow from the leak valve. All steps will be automated. Said gas burst is made available by gating a measured volume of gas with a small solenoid valve, pulsed open for approximately 18 msec.

Operation and Results

Ion Source Performance

A gas flow 20 times greater than normal is helpful for quickly obtaining the heat necessary to alter the normally positive resistance characteristic of pulsed arcs with high melting point materials, to a negative resistance. This condition becomes mandatory when the voltages available are minimized. Supranormal magnetic fields also permit the arc to "strike" at lower arc voltages (Fig. 17). Under ideal conditions, with minimal cooling, this arc can be struck with 1200 V. Usually, however, 4 kV and currents of some fraction of an ampere are needed to heat the cathodes at which time the power supply is switched to the 1.0 kV, 2-6 A mode. Depending upon the rate of temperature rise of the cathodes, 3-15 sec of starting-mode operation is required every time the arc is shut off and cools. Hence, automatic, rapid gas control is needed to avoid this lengthy starting procedure arising from unforeseen ion source operation at subnormal gas flows.

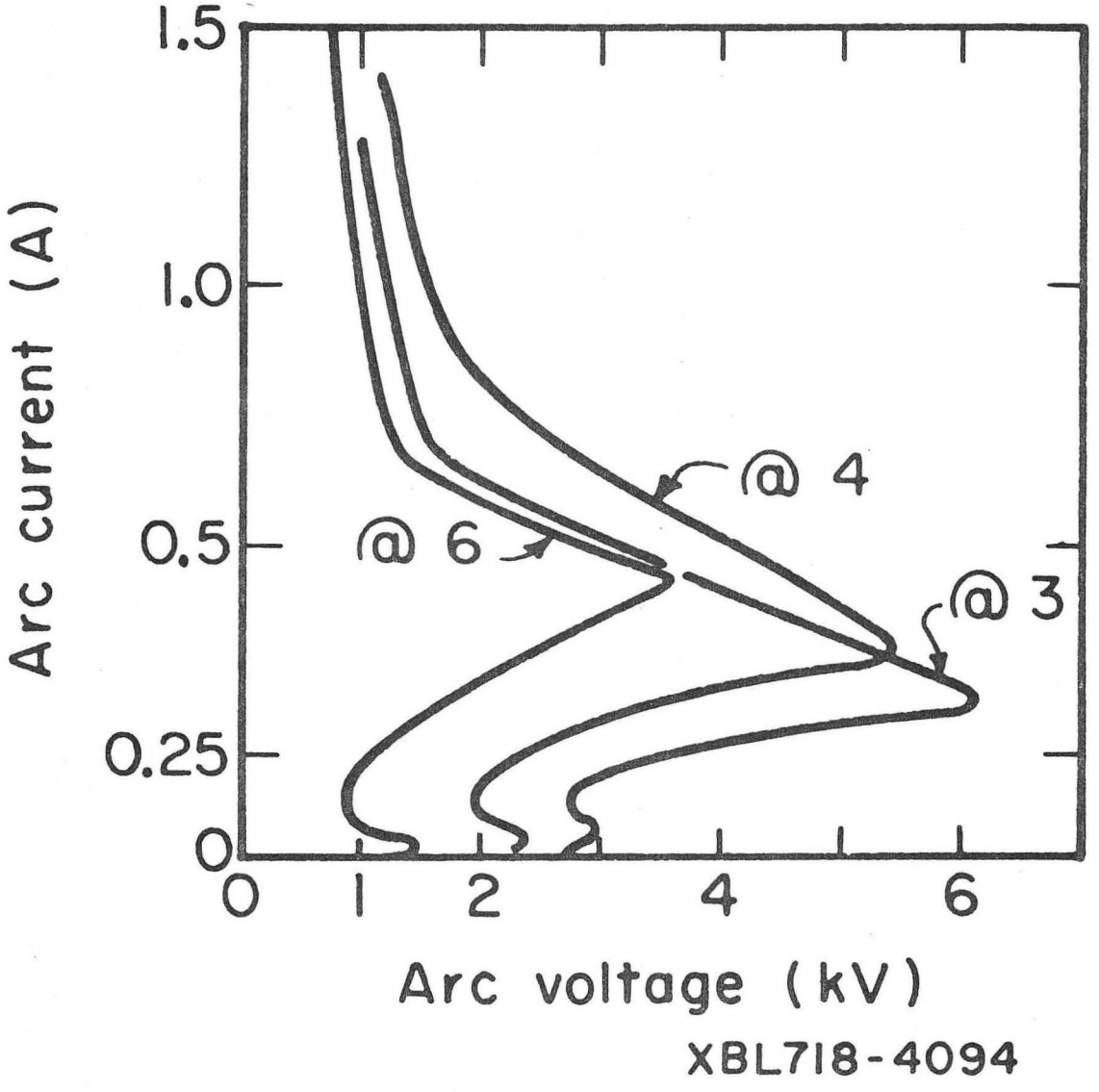

Fig. 17. Time-independent, simultaneous plot of arc voltage and current. (Units of magnetic field are arbitrary.)

Typical "high current mode" arc characteristics are shown in Fig. 18. This arc will not sustain itself in general at fields less than 2.0 kG on the source axis. As the cathodes sputter, tantalum builds up on removable anode end pieces, flared to receive this material without immediate constriction of the bore. Gas flows must be raised, and beam levels are lowered by this constriction if it continues. Anode ends and cathodes are replaced every 6 hr when running a 5-A argon arc.

A limited test of an ion source similar to that described here has been run in a 180° mass spectrometer. Conclusions reached show that a linear relationship exists between arc current and a $^{40}Ar^{4+}$ beam, and that a doubling of arc power leads to an increase of the beam by a factor of 3.2 (Fig. 19). This arc produces approximately 54 mA/em^2/kW (or 30 mA/cm^2/A), when 20 kV above ground. Information about charge state distribution was unattainable since beam energy, by necessity, had to be a variable in this spectrometer.

150 μA of Kr^{5+} ions have been measured 6 ft downstream from the HV terminal magnet, in a large Faraday cup where the highest pressure of the system was 13 μtorr. This was done at 32% duty factor with the arc at 4A, 770 V, and the extractor at 25 kV. In general, a doubling of the pressure along the beam path will lower $^{84}Kr^{5+}$ beam levels, as measured at this cup, from one-half to one-seventh. This ratio increases at lower pressures, demonstrating the importance of good vacuum (Fig. 20).

Preliminary calorimetric measurements indicate that approximately 6 mA of total (peak) ^{40}Ar beam enters the analyzing section of the magnet when 1 mA of $^{40}Ar^{3+}$ exits the magnet (extractor at 15 kV). Beam levels of $^{40}Ar^{2+}$ as a function of extractor voltage are shown in Fig. 21.

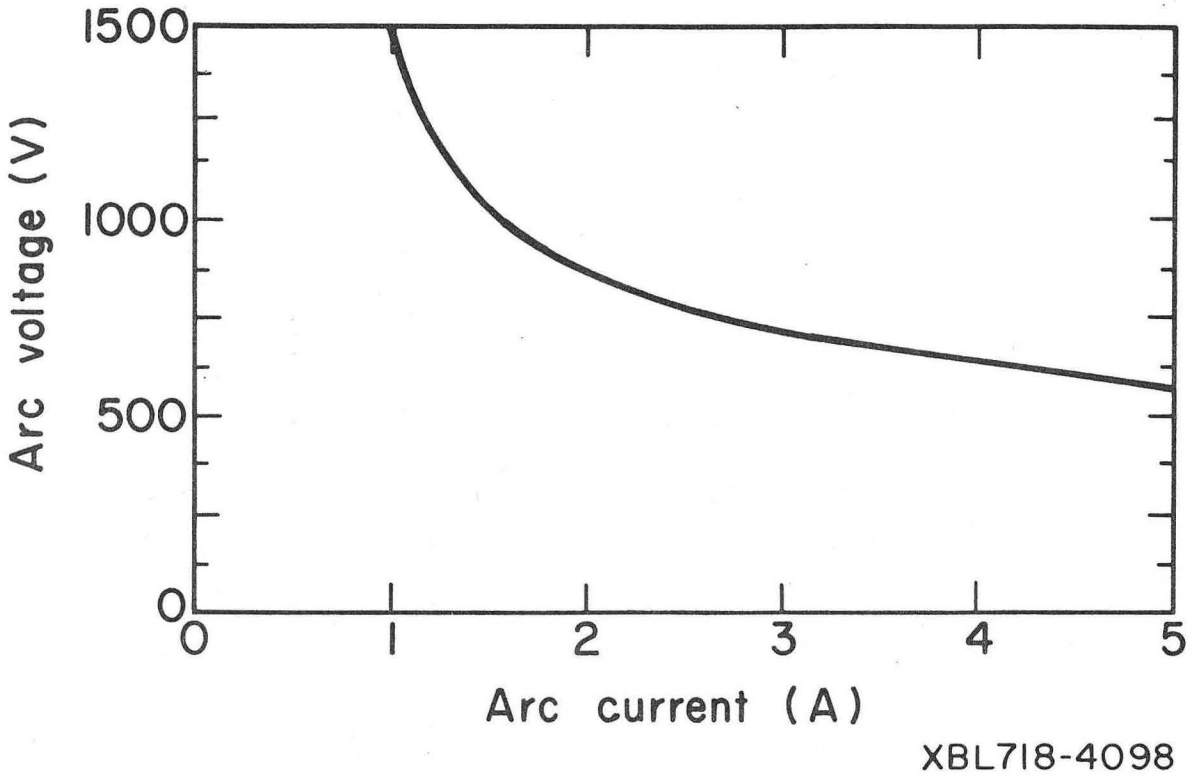

Fig. 18. High-current mode arc operating characteristics.

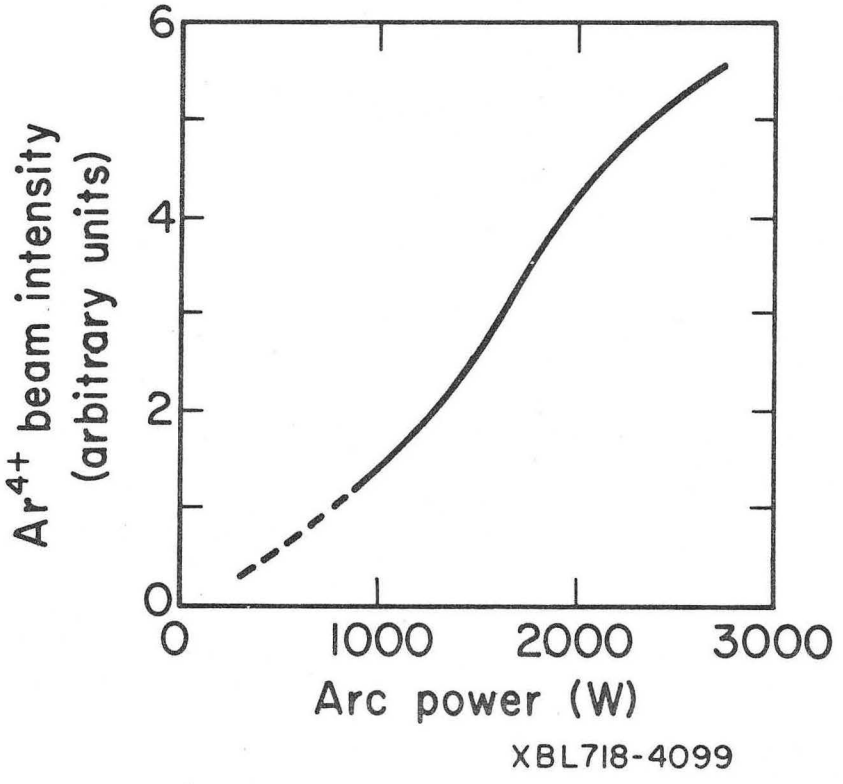

Fig. 19. Beam intensity plotted as a function of arc power.

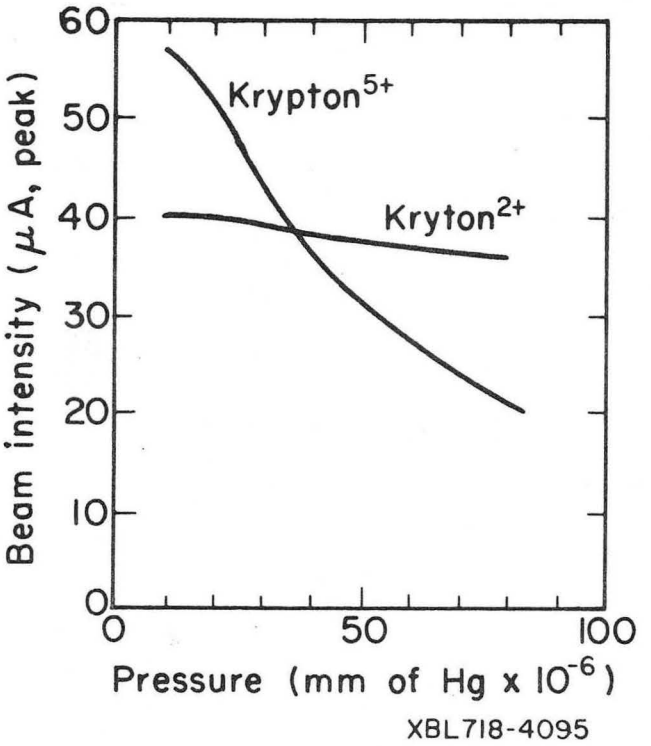

Fig. 20. Beam intensity plotted as a function of vacuum pressure in the terminal transport system.

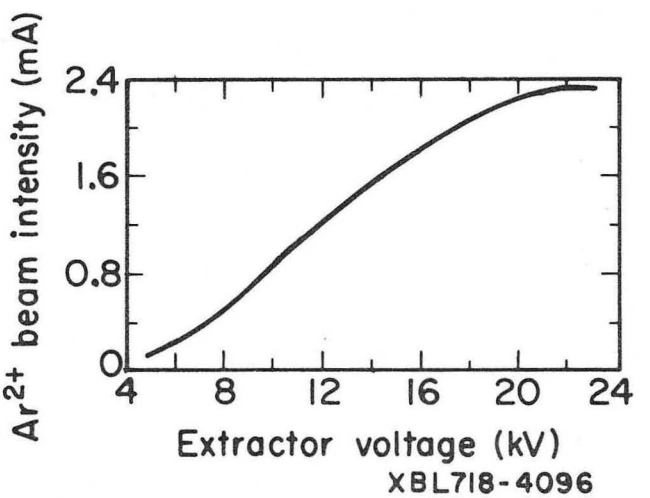

Fig. 21. $^{40}A^{2+}$ beam intensity as a function of extractor voltage.

Beam Dynamics and Experimental Results

To get answers to some of the problems we encountered while building the beam transport system within the strict weight, volume, and power limitations, a prototype analyzing magnet was constructed for early beam optics studies before commitment to a final design. This workbench setup also allowed the ion source to be tested, as well as other transport devices, the vacuum system, and various power supplies. The final beam parameters were chosen with the additional aid of ray-tracing computations performed by two computer programs.

In order to minimize the ampere-turns requirement of the source magnet and at the same time provide reasonable charge-state separation after analysis, the radius of curvature was chosen as 5.6 in. The beam leaves the extractor within a divergence half-angle of 12° and travels approximately 2.5 in. within the low-field region before entering the analyzing gap. Figure 22 shows the ion source in the magnet with the top pole removed.

The beam is pulled from the source anode through an extractor slit 0.070 in. wide (radially) by 0.65 in. high (axially), is analyzed through a total turning angle of 129°, and crosses the magnet exit edge with an effective field edge angle of 32°. The extractor-anode spacing is typically 0.070 in. The pole exit edge has no curvature to provide second-order correction; however, the proximity of the tape-wound coils and the narrow width provide some curvature to the profile of the effective edge. All but a small percent of the selected charge-state beam traverses the analyzing magnet within 98% of the central field values, using flat pole faces. Ray-tracing calculations have shown that shaping the pole edges along the analyzing path to provide an absolutely flat transverse field profile would yield no substantial increase in beam quality.

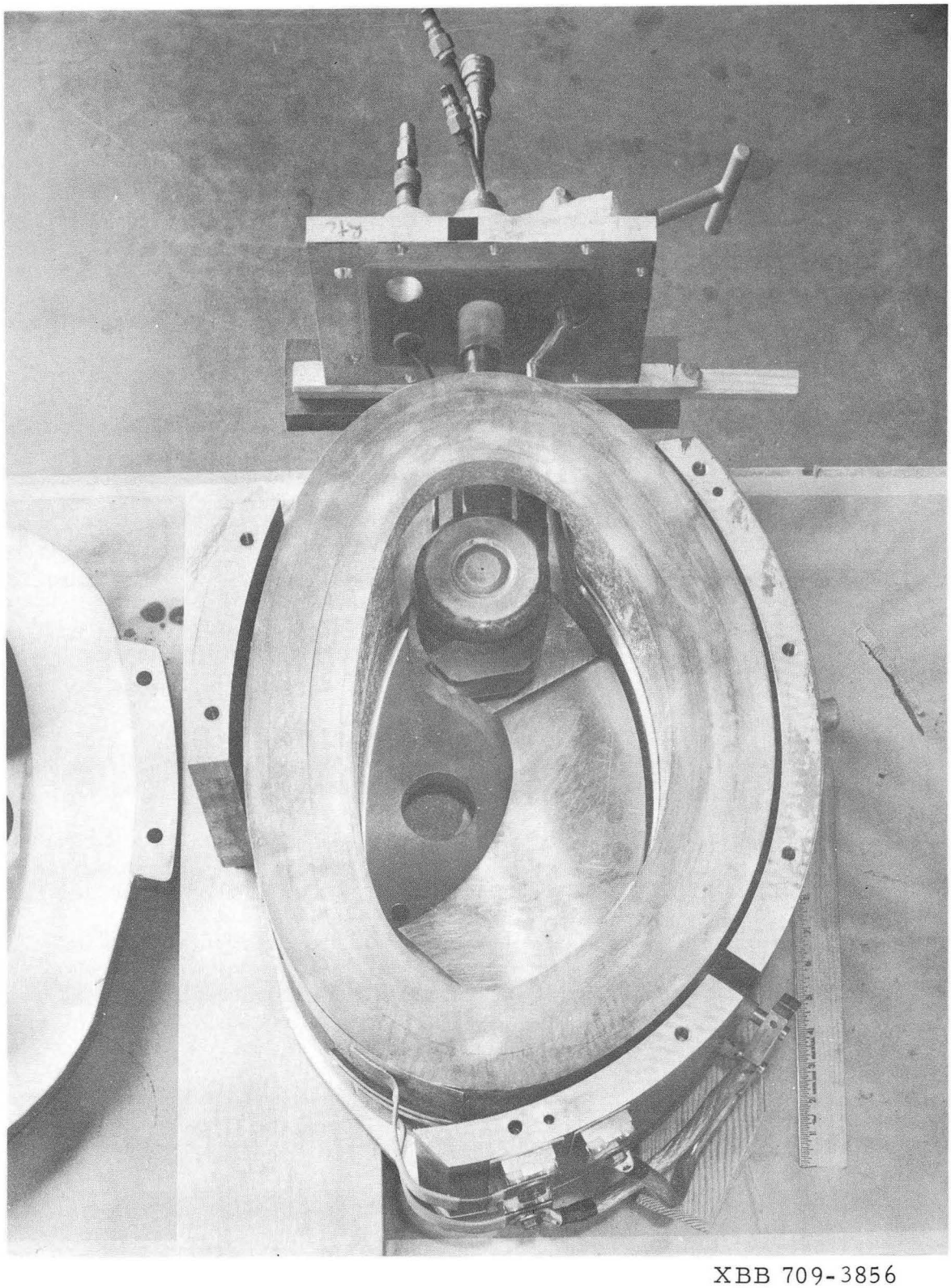

XBB 709-3856

Fig. 22. Ion source mounted in the magnet with the top pole removed.

Any change in source angle, extractor position, or ion energy can give different focal properties to the source beam. Consequently, a quadrupole doublet is necessary to insure reproducible focal properties of the system. Each lens is capable of operating well above the specified strength of 7 kG ($B' \times L_{eff}$), with less than 0.13% of the n = 3 component at a radius of 1 in. Calculations show a modest power level will normally be used.

A vernier magnet, capable of bending the most rigid beam through $\pm 3^{\circ}$, is included in the transport system to insure that the particles can be adjusted parallel to the HV column axis in the radial plane. It is located at the approximate beam waist location, 18 in. downstream from the analyzing magnet. Axial alignment is accomplished by the mechanical precision with which the components are mounted together, and no other adjustment is provided.

Beam monitoring in the HV terminal under operating conditions is done with a flip-type Faraday cup. It is mounted next to the vernier magnet, so that advantage may be taken of the stray field to suppress secondary electron emission from the cup. In front of the cup is a 0.5-in.-wide beam slit, electrically isolated from ground, which helps reject unwanted charge states transmitted by the analyzing magnet. It also is used as a noninterrupting beam monitor.

Radial and axial emittance of the beam was determined with a collimator assembly containing an adjustable slit and a scanning slit separated by a known distance, followed by a large Faraday cup. The emittances measured at the entrance of the accelerating tube are shown in Fig. 23. To improve the acceptance of the accelerating tube the entrance gradient has been lowered along the first 10% of its length to about one-third the normal value.

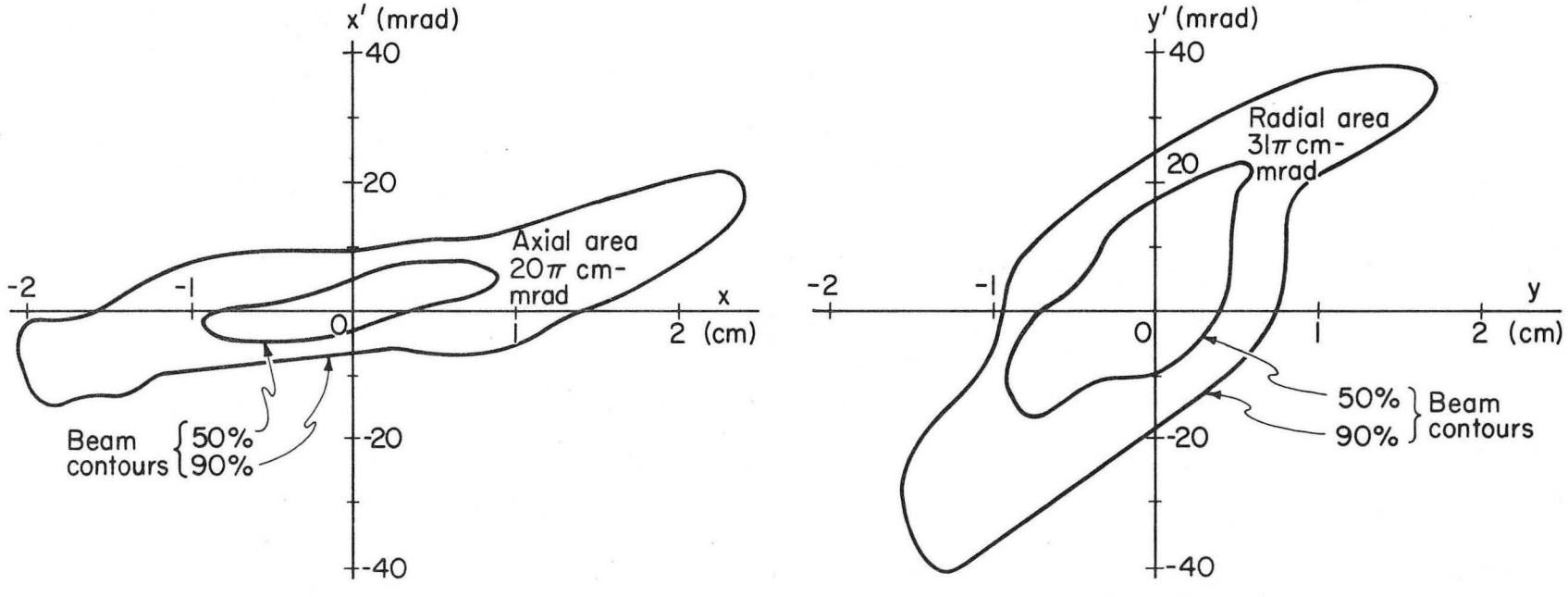

Fig. 23. Beam emittance at the accelerating tube entrance.

Argon beams were used for most of the beam dynamics experiments because the charge states in the range of acceptable e/m ratios are completely separable by the analyzing magnet. The results were therefore not ambiguous because of charge-state overlap. Those beams whose charge states result in e/m ratios differing by less than 10% will not be completely analyzed by the injector, and they will undergo further selection by the ground-end transport system and the linac itself.

Input to the prestripper tank requires that the particles have a $\beta = 0.01548$. For the $^{238}U^{10+}$ (e/m = 0.042) beam this means a terminal voltage of about 2.68 MV and a corresponding value of almost 1.25 MV for a particle with e/m = 0.09. Most of our investigations of the accelerated beam at the ground end have been conducted at or below the last mentioned voltage to limit the x-ray hazard to the operating personnel.

Footnote and References

*Work done under the auspices of the U. S. Atomic Energy Commission.

1. M. Schenkel, A. New Wiring Arrangement for the Production of High Potential, Electrotech. Z. 40, 333 (1919).

2. H. Greinacher, Ueber eine neve Methode, Wechselstrom mittels elektrischer Ventile und Kondensatoren in hochgespannten Gleichstrom zu verwandeln, Z. Physik 1 (1921).

3. Marshall R. Cleland and Paul Farrell, Dynamitrons of the Future, IEEE Trans. Nucl. Sci., June 1965, p. 277.

4. L. L. Reginato et al., PCM Telemetry System for the 3-MV SuperHilac Injector, Lawrence Radiation Laboratory Report UCRL-20179, March 1971.

5. Consolidated Vacuum Corp. Ionization Gage Tube-Type VG-1A, Bulletin No. 9-55.

TECHNICAL INFORMATION DIVISION
LAWRENCE BERKELEY LABORATORY
UNIVERSITY OF CALIFORNIA
BERKELEY, CALIFORNIA 94720